Combined Teletraffic/Transmission Analysis of a Transparent Space-Division Optical Star Network

Alberto Bononi
Dipartimento di Ingegneria dell'Informazione – Università di Parma – Parma, Italy

ABSTRACT The combined teletraffic-transmission analysis of a single-wavelength cell-switching all-optical local area network (LAN) with star topology is presented. The star is a multistage space-division photonic switch that uses deflection routing. Deflected packets delivered to the wrong user are transparently rerouted to the switch. Each time a packet crosses the central switch, it collects amplifier noise and crosstalk due to imperfect optical switching. As the network load increases, the crosstalk level per crossing increases, as well as the number of crossings caused by deflections. The traffic statistics hence strongly affect the quality of the received signals. It is found that such networks work well only when lightly loaded. Using fast optical transmitters and receivers to deplete the optical layer has the positive effect of reducing both deflections and crosstalk, while allowing simpler architectures at the optical level.

1 Introduction

A major advantage of transparent optical networks is the possibility of flexibly upgrading the transmission rates and hence the network capacity by upgrading only transmitters and receivers at the access nodes, leaving the core of the network untouched. Such an advantage in management is also a major weakness in transmission. Transparency implies non-regenerative (or analog) transmission from source to destination, with the ensuing degradation of the quality of signals due to accumulation of noise and distortion.

Amplified spontaneous emission (ASE) noise and switch-induced coherent crosstalk are the two major transmission impairments in high-speed single-wavelength transparent optical LANs [1].

In a cell-switching environment with dynamic routing, it is essential that cell paths be limited to a small number of hops, since each hop entails large power losses, accumulation of ASE and crosstalk. It has been shown in [2] that intrinsically multihop two-connected topologies, such as Shufflenet, present much larger total power losses than centralized networks, particularly when the loss of the alignment stages (optical elastic buffers) are considered. Thus topologies that have on average a few hops are ideal candidates for transparent networks employing deflection routing. Here we present and analyze one of such centralized networks.

Section 2 introduces the network model, Section 3 derives the teletraffic statistics of the network in uniform traffic, Section 4 derives the packet error rate for a fixed path in the network, while Section 5 uses the results of Sections 3 and 4 to compute the average packet error rate, taking into account the transmission characteristics of the optical components. Section 6 concludes the paper.

0-7803-3336-5/96 $5.00 © 1996 IEEE

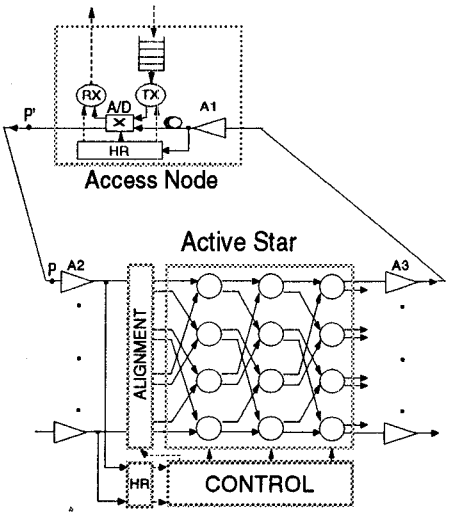

Figure 1: Star Network architecture

2 Network Model

The proposed network, shown in Fig. 1, is an MxM space-division cell switch (Active Star) to which M access nodes are connected by dedicated fibers.

Each node is equipped with an optical transmitter (TX) and an optical receiver (RX), and has an electronic input buffer to store incoming cells.

The header recognition block (HR) taps power off both at the access node and at the star to electronically read the cell headers and make routing/control decisions.

Cells are aligned at the star by tunable optical delays.

In our analysis, the active star is a multistage photonic switch, with $\log_2 M$ Shuffle Exchange (SX) stages based on crossbar directional couplers.

The elementary 2x2 β-elements within the active star (shown with circles in Fig. 1) are either composed of a single crossbar (*1c* β-element), or of two crossbars with a one-cell fiber delay loop sandwiched in between acting as a 1-cell optical buffer (*2c* β-element) [3].

Each β-element is controlled based only on the destinations of packets at its inputs (and possibly present in its buffer) using deflection routing [4]. Deflection routing is used because en-route transparent optical buffering at the interconnect cannot easily be provided, since as we will see it introduces large power losses and crosstalk. Interconnects without buffers and with a single buffer per β-element only will be compared, since it is known that in uniform traffic a single buffer is enough to route packets almost as efficiently as with infinitely many buffers [5].

Deflected packets are delivered to the wrong user and transparently re-routed to the interconnect. The network, which is intrinsically single-hop, becomes gradually multi-hop as deflections take place.

3 Teletraffic Analysis

Suppose the offered traffic is uniform, i.e., each node receives from the outside a stream of independent packets uniformly destined to all other nodes in the network. Let the average arrival rate at each node be T packets/slot. At most one packet can be injected in the optical layer per slot, and packets recirculating from the star are given priority over local packets. As long as the input electronic buffers – which we suppose of infinite size – are not saturated, T is the throughput per node. Let u be the slot utilization, i.e., the probability that a slot carries a packet. Given the symmetry of the network, u is the same for all slots.

If H is the number of hops (i.e., interconnect crossings) that a packet on average undergoes before reaching its destination, a simple application of Little's law gives:

$$T = \frac{u}{H}. \tag{1}$$

Since u is the average number of packets/slot that reach the interconnect on each input, and T is the average number of packets/slot that successfully reach each destination, $d \triangleq (u-T)/u$ is the fraction of deflected packets, i.e., the deflection probability per input port at the interconnect.

Packets reach the central interconnect, aligned in an array of M input slots per clock. If m packets at the input slots compete for the same destination, one of them reaches such destination, while the remaining $(m-1)$ loop back and try again. If all roundtrip delays correspond to different multiples of the slot time, deflected packets always meet new packets at the interconnect. Hence the number of hops h taken by a typical packet before reaching its destination follows a geometric distribution:

$$p_h(n) \triangleq Pr[h=n] = (1-d)d^{n-1}. \tag{2}$$

since the packet hops n times if it is deflected $n-1$ times and makes it at the n-th trial, all trials being independent.

It is possible to derive an expression of the throughput as a function of u. Assuming that packets at the input slots have uniformly distributed destinations the throughput T_S of an unbuffered (1c) interconnect with $S = log_2 M$ stages is found by the following recursive formula [2]:

$$\begin{cases} T_0 &= u \\ T_k &= 1-(1-T_{k-1}/2)^2, \quad k=1,..,S \end{cases} \tag{3}$$

A similar expression is obtained for the single-buffer case (2c) [2]:

$$\begin{cases} T_0 &= u \\ T_k &= T_{k-1}\left(1-\frac{(\frac{1}{2}T_{k-1})^3}{1-T_{k-1}+T_{k-1}^2}\right) \quad k=1,..,S \end{cases} \tag{4}$$

Fig. 2 shows the average number of hops H and the link load u vs. throughput, obtained from (1), (3), and (4), in uniform traffic for M=256 nodes. The average number of hops does not exceed 3.5 for the unbuffered (*1c*) case, and is below 2 for the buffered (*2c*) case. Increasing the throughput causes an increase of the number of hops, hence more power losses and crosstalk. Also shown is the increase with throughput of the link load, i.e. of the fraction of nonempty slots, which causes an increase of the coherent crosstalk in the active star. Circles show simulation results, which are in good agreement with the theoretical formulae.

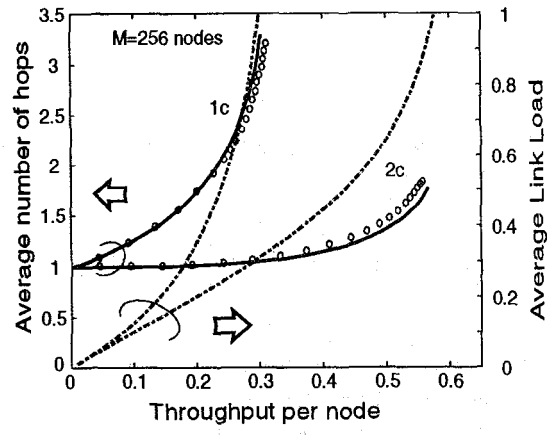

Figure 2: Average number of hops and link load vs throughput in uniform traffic. 1c = no buffer, 2c = single-buffer.

4 Transmission Analysis

This section will derive the bit error rate $BER(n)$ of a packet that has hopped n times before reaching its destination. All symbols of interest are given in Table I, along with the values used in the analysis.

Packets are On/Off keying (OOK) modulated with non-return-to-zero (NRZ) pulses at a bit rate $R = 1/T$, where T is the bit time, at an optical carrier frequency $\nu_0 = \omega_0/2\pi$.

The direct-detection receiver consists of a bandpass optical filter of bandwidth $B_o = m_{exp} R$ centered at the carrier frequency ν_0 (where m_{exp} is the bandwidth expansion factor), a polarization filter, a photodiode (PD), and a matched (integrate-and-dump) filter, followed by a sampler and by the decision circuitry [6].

We fix the attention on a *test* bit taking n hops and reaching its intended receiver. It collects crosstalk at the interconnect and ASE noise in the optical amplifiers. The objective is to find the probability of error on such a bit.

To simplify the transmission analysis, links from the node to the star are assumed to have the same length Δ [1], and cells are assumed to be bit-aligned at the star, which simplifies the crosstalk computations. Packets at all transmitters have the same power P_{tx} on mark and zero power on space.

Doped-fiber amplifiers A_1, A_2, A_3 are placed as in Fig. 1. We assume the amplifiers are identical, have maximum gain G_M and saturation power P_{sat}. The equivalent input ASE added at each amplifier is modeled as an additive white gaussian noise (AWGN) process with (one-sided) power spectral density $N_0 = h\nu_0 n_{sp}(G-1)/G$, where h is Planck's constant, n_{SP} is the spontaneous emission factor, and G is the power gain [7]. An optical filter of bandwidth B_o centered at ν_0 is supposed to follow each amplifier to prevent saturation due to ASE.

To keep equal power levels in the network, the amplifiers are set

[1] At high bit rates, link lengths are large multiples of the slot time. Therefore link lengths may differ in number of slots, which justifies (2),(3),(4), but be very close in value.

Symbol	Meaning	Value/Range
M	# of nodes	256
u	link load	$\in [0,1]$
n	# of hops	
R	bit rate (b/s)	
m_{exp}	bandwidth expansion factor	5
Δ	node-star fiber span	10 Km
P_{tx}	transmitted mark power	0 dBm
n_{sp}	EDFA spontaneous emission factor	1.3
G_M	EDFA maximum gain	30 dB
P_{sat}	EDFA output saturation power	6 dBm
L_{hr}	header recognition tapping loss	1 dB
L_{ad}	add/drop coupler loss	3 dB
L_n	access node loss	$L_{hr} * L_{ad}$
L_f	fiber loss (over Δ Km)	2.5 dB
L_{al}	alignment loss	10 dB
s	# of couplers crossed in the interconnect	$\log_2 M$ when $\beta = 1c$ $2 * \log_2 M$ when $\beta = 2c$
L_{ic}	interconnect loss	2*s dB
L_s	total loss at the star	$L_{hr} * L_{al} * L_{ic}$
α	switch crosstalk factor	-30 dB
n_{xt}	# of crosstalk interferers	$ns + 2$
$\mathcal{R}$	photodiode responsivity	1 A/W
$k_B T$	(Boltzman const.)*(temperature)	4.14 x10^{-21} W/Hz
C	Input capacitance	0.2 pF
q	Electron charge	1.6 x 10^{-19} C
N_b	# bits/cell	1000

Table 1: Parameters used in calculations.

to have unity roundtrip gain

$$G_1 G_2 G_3 = L_n L_f^2 L_s \tag{5}$$

where the losses are defined in Table 1. With this assumption, packets at the star have all the same power level, and therefore the crosstalk accumulated at each pass does not depend on the gains (G_1, G_2, G_3). It is therefore possible to choose (G_1, G_2, G_3) to minimize BER(n), by minimizing the accumulated ASE power at the receiver.

4.1 Gain Optimization

With the aid of Fig. 1, the ASE power density accumulated by the test bit in *one* hop from point P to P' is seen to be

$$N_{ase}(1) = h\nu n_{sp}\left[\frac{(G_2-1)G_3G_1}{L_sL_fL_n} + \frac{(G_3-1)G_1}{L_fL_n} + \frac{G_1-1}{L_n}\right]$$

since the ASE processes are independent. Using (5) to eliminate G_2 gives

$$N_{ase}(1) = h\nu n_{sp}L_f\left[1 - \frac{1}{L_nL_f} + \frac{G_1G_3(L_s-1)}{L_sL_f^2L_n} + \frac{G_1(L_f-1)}{L_f^2L_n}\right]. \tag{6}$$

Given constraint (5), such noise contribution remains constant until absorption, and each hop contributes the same noise level, so that $N_{ase}(n) = nN_{ase}(1)$. This is the quantity to be minimized, subject to gain constraints $1 \le G_i \le G_M$, $i = 1,2,3$, and to saturation constraints:

$$\begin{aligned} P_{o1} &\triangleq \frac{P_{tx}}{L_{ad}}L_n &&\le P_{sat} \\ P_{o3} &\triangleq P_{o1}\frac{L_f}{G_1} &&\le P_{sat} \\ P_{o2} &\triangleq P_{o3}\frac{L_s}{G_3} &&\le P_{sat} \end{aligned} \tag{7}$$

where P_{oi} is the output power of amplifier A_i, $i = 1,2,3$. The Appendix derives the optimum gains (G_1, G_2, G_3).

4.2 Crosstalk Analysis

The desired OOK signal s_0 at the input of the interconnect during the *test* bit can be expressed as

$$s_0 = \Re\left\{\sqrt{2P_m}\, m_0 e^{j\omega_0 t}\right\} \quad (\sqrt{\text{Watt}}) \tag{8}$$

where P_m is the mark power, $m_0 \in \{0,1\}$ is the modulation bit, and $\Re\{z\}$ indicates the real part of z.

The remaining $M-1$ signals at the input of the interconnect are given as $s_i = \Re\{\tilde{s}_i \exp(j\omega_0 t)\}$, $i = 1, ..., M-1$. The complex envelope $\tilde{s}_i$ can be expressed as

$$\tilde{s}_i = \sqrt{2P_m}\, m_i\, X_i\, Y_i\, e^{j\phi_i} \tag{9}$$

where:

1) m_i are the modulation bits, independent identically distributed (IID) random variables (RV), taking value 1 or 0 with equal probability;

2) X_i are IID RVs taking value 1 or 0 with probability u and $1-u$ respectively. They specify whether or not a packet is present on the corresponding input slot;

3) a polarization filter at the receiver is assumed to filter away the components orthogonal to the desired signal. $Y_i \triangleq \cos\psi_i$ are the polarization projections of the i-th field along the polarization direction of the test signal. The angles ψ_i are assumed to be IID RVs, uniform over $[-\pi, \pi]$. Although a practical receiver will not keep track of the desired signal's polarization state, neglecting orthogonal (non-coherent) components has little impact on performance, since the crucial crosstalk contribution is the *coherent* beat with the signal;

4) ϕ_i are IID RVs, uniform over $[-\pi, \pi]$ and constant over the bit time T. They account for phase noise at the TX laser, unequal propagation delay to the interconnect and other possible sources of phase instability.

Eq. (9) models the case of uncorrelated, externally modulated laser sources for the case in which laser linewidth is much smaller than the modulation rate, in the worst-case scenario of coinciding optical carriers.

Crosstalk arises from incomplete switching in the 2x2 directional couplers within the interconnect. If P_{in} is the power at one input of the coupler, the power at the low-attenuation (i.e., the desired) output is $P_{out}^L = (1-\alpha)P_{in}/L_c$, while the power at the high-attenuation port (i.e., the one leaking undesired power) is $P_{out}^H = \alpha P_{in}/L_c$. L_c represents the coupler loss, and α is the crosstalk factor.

As the *test* bit crosses the couplers at each stage of the interconnect, it collects crosstalk from the optical fields simultaneously crossing the same couplers. Since $\alpha \ll 1$, only first-order crosstalk terms will be considered.

At the output of the interconnect, the complex envelope of the optical field (relative to the desired signal frequency ν_0) at the test bit time is

$$\tilde{e}_o = \sqrt{\mathcal{A}}\left[m_0 + \sqrt{\frac{\alpha}{1-\alpha}}\sum_{i=1}^{s} d_i\, e^{j\phi_i}\right] \tag{10}$$

where

$$\begin{aligned} \mathcal{A} &\triangleq 2P_m[(1-\alpha)/L_c]^s = 2P_m/L_{ic} \\ d_i &\triangleq m_i\, X_i\, Y_i\,. \end{aligned} \tag{11}$$

Equation (10) shows that the test bit crosses s couplers in low-attenuation and has thus power loss proportional to $(1-\alpha)^s$,

while the first-order crosstalk terms cross all but one stage in low-attenuation, so that their power loss is proportional to $(1-\alpha)^{s-1}\alpha$. The value of s is $\log_2 M$ in the case of $1c$ β-elements, and $2\log_2 M$ in the case of $2c$ β-elements. For $2c$ β-elements we approximate to u the probability that the buffer is full.

After n hops, due to the unity feedback gain, the signal power plus crosstalk can still be expressed by (10), where the upper limit in the summation must be changed from s to $n\,s$. The $n\,s$ crosstalk interferers will be assumed to be independent RVs, although some packets may interfere with the test packet more than once. By using (10) we implicitly assume that all interfering packets have the same nominal power level P_m, and thus neglect the random accumulation of crosstalk and ASE on each packet in the calculation of the crosstalk on the test bit.

Crosstalk may arise even at the add/drop switch during injection and absorption of the packet, adding two more crosstalk terms.

4.3 Photodetection

From the results of the previous subsections, the complex envelope of the field at the photoreceiver after n hops can be approximated as

$$\tilde{e}_{rx} = \sqrt{2P_{rx}}\left[m_0 + \sqrt{\frac{\alpha}{1-\alpha}}\sum_{i=1}^{n_{xt}} d_i\, e^{j\phi_i}\right] + \tilde{n}_{\mathrm{ASE}}(t) \qquad (12)$$

where the received power for mark bits is, by the unity feedback gain constraint, $P_{rx} = P_{tx}/L_{ad}$, and $n_{xt} \triangleq ns + 2$ is the number of crosstalk interferers. $\tilde{n}_{\mathrm{ASE}}(t)$ is the complex envelope of the accumulated ASE, which is an additive gaussian bandpass process of flat one-sided spectral density $N_{ase}(n)$ over the optical filter bandwidth B_o.

The current after the photodetector is

$$i(t) = \frac{\mathcal{R}}{2}|\tilde{e}_{rx}(t)|^2 + i_{sn}(t) + i_{th}(t) \qquad (13)$$

where $\mathcal{R}$ is the responsivity of the photodetector (Ampere/Watt), $i_{sn}(t)$ is the shot noise current, and $i_{th}(t)$ is the thermal noise of the electronic circuitry.

The first term in (13) can be written as

$$\begin{aligned} I_p(t) &= (\mathcal{R}/2)(\tilde{e}_{rx}(t)\tilde{e}^*_{rx}(t)) = \\ &= \mathcal{R}P_{rx}\left\{m_0 + x_{s-xt} + x_{s-sp} + x_{xt-xt} + x_{xt-sp} + x_{sp-sp}\right\} \end{aligned} \qquad (14)$$

where the asterisk denotes complex conjugation, and where the contributions of the beat terms between signal and crosstalk (s-xt), signal and ASE (s-sp), crosstalk with itself (xt-xt), crosstalk with ASE (xt-sp), and ASE with itself (sp-sp) can be written after some algebraic manipulations as

$$\begin{aligned} x_{s-xt} &= 2m_0\sqrt{\tfrac{\alpha}{1-\alpha}}\textstyle\sum_{i=1}^{n_{xt}} d_i\cos(\phi_i) \\ x_{s-sp}(t) &= 2m_0 n_i(t) \\ x_{xt-xt} &= \tfrac{\alpha}{1-\alpha}\textstyle\sum_{i=1}^{n_{xt}}\sum_{k=1}^{n_{xt}} d_i d_k\cos(\phi_i-\phi_k) \\ x_{xt-sp}(t) &= 2\sqrt{\tfrac{\alpha}{1-\alpha}}\textstyle\sum_{k=1}^{n_{xt}} d_k\left[n_i(t)\cos(\phi_k) + n_q(t)\sin(\phi_k)\right] \\ x_{sp-sp}(t) &= n_i^2(t) + n_q^2(t). \end{aligned} \qquad (15)$$

In (15), $\tilde{n}(t) \triangleq \tilde{n}_{\mathrm{ASE}}(t)/\sqrt{2P_{rx}}$ is the normalized ASE noise, while n_i and n_q are its real and imaginary part, respectively. The spectrum of $n_{\mathrm{ASE}}(t)$ is a gate centered around ν_0, so that $n_i(t)$ and $n_q(t)$ are independent gaussian lowpass processes with (two-sided) spectral density level $\widehat{N_{ase}}(n) \triangleq N_{ase}(n)/(2P_{rx})$, constant over $[-B_o/2, B_o/2]$, and zero outside.

Let $x_{sn}(t) \triangleq i_{sn}(t)/\mathcal{R}P_{rx}$ and $x_{th}(t) \triangleq i_{th}(t)/\mathcal{R}P_{rx}$. The normalized statistic at the decision gate can be expressed as

$$Z = \left(\frac{1}{\mathcal{R}P_{rx}}\right)\frac{1}{T}\int_0^T i(t)\,dt = m_0 + Y \qquad (16)$$

where the signal-dependent noise term Y is a sum of uncorrelated contributions

$$Y = Y_{s-xt} + Y_{s-sp} + Y_{xt-xt} + Y_{xt-sp} + Y_{sp-sp} + Y_{sn} + Y_{th} \qquad (17)$$

where each noise term takes the form $Y_{\square} = \frac{1}{T}\int_0^T x_{\square}(t)dt$.

As the number of IID crosstalk interferers n_{xt} gets large, the distribution of each crosstalk-dependent term in (15) tends, by the central limit theorem, to a gaussian RV. Hence the crosstalk contribution to the noise term Y tends to a gaussian RV, and the BER can be approximated by a gaussian formula, which has already been shown to give accurate results in the absence of crosstalk [8]–[9].

In the gaussian approximation, $BER(n) = Q(\gamma)$ [8], where

$$\gamma \triangleq \frac{E[Z/m_0=1] - E[Z/m_0=0]}{\sigma[Z/m_0=1] + \sigma[Z/m_0=0]} \qquad (18)$$

where $E[\bullet]$ denotes expectation, and $\sigma[\bullet]$ denotes standard deviation.

It is now a matter of finding mean and variance of Z as the sum of the mean and variance of each component in (17). After some algebra, one finds that the only nonzero mean values are: $m_{xt-xt} = \frac{\alpha}{1-\alpha}\frac{un_{xt}}{4}$, and $m_{sp-sp} = 2m_{exp}\widehat{N_{ase}}(n)R$. The variances are:

$$\begin{cases} \sigma^2_{s-xt} &= m_0\frac{\alpha}{1-\alpha}\frac{un_{xt}}{2} \\ \sigma^2_{s-sp} &= 4m_0\widehat{N_{ase}}(n)R \\ \sigma^2_{xt-xt} &= \left(\frac{\alpha}{1-\alpha}\right)^2\frac{un_{xt}}{16}(3+u(n_{xt}-2)) \\ \sigma^2_{xt-sp} &= \frac{\alpha}{1-\alpha}un_{xt}(\widehat{N_{ase}}(n)R) \\ \sigma^2_{sp-sp} &= (4m_{exp}-1)(\widehat{N_{ase}}(n)R)^2 \\ \sigma^2_{sn} &= \frac{qR}{\mathcal{R}P_{rx}}(m_0 + m_{xt-xt} + m_{sp-sp}) \\ \sigma^2_{th} &= \left(\frac{1}{\mathcal{R}P_{rx}}\right)^2 2\pi(k_B\tau)CR^2 \end{cases} \qquad (19)$$

The dominant terms are by far the beat terms (s-xt) and (s-sp).

5 Combining Teletraffic and Transmission

Assuming cells of N_b bits and errors independent bit by bit, the unconditional packet error rate is obtained by conditioning on the number of hops n taken by a typical packet in the network as

$$PER = \sum_{n=1}^{\infty}[1-(1-BER(n))^{N_b}]p_h(n) \qquad (20)$$

where $p_h(n)$ is given in (2).

The system parameters used in the results are given in Table 1, unless otherwise noted.

Fig. 3 shows PER curves with load u as a parameter. Fig 3(a) shows the variation with bit rate R, for a fixed crosstalk factor $\alpha = -30dB$, while Fig. 3(b) is plotted versus α, with $R = 2.5Gb/s$. Dotted lines refer to $1c$ β-elements, and solid lines to $2c$ β-elements. Curves for $1c$ in Fig. 3(a) weakly depend on bit rate, which means that signal-crosstalk beat (which, as seen from (19), is bit rate independent) is the dominant noise component.

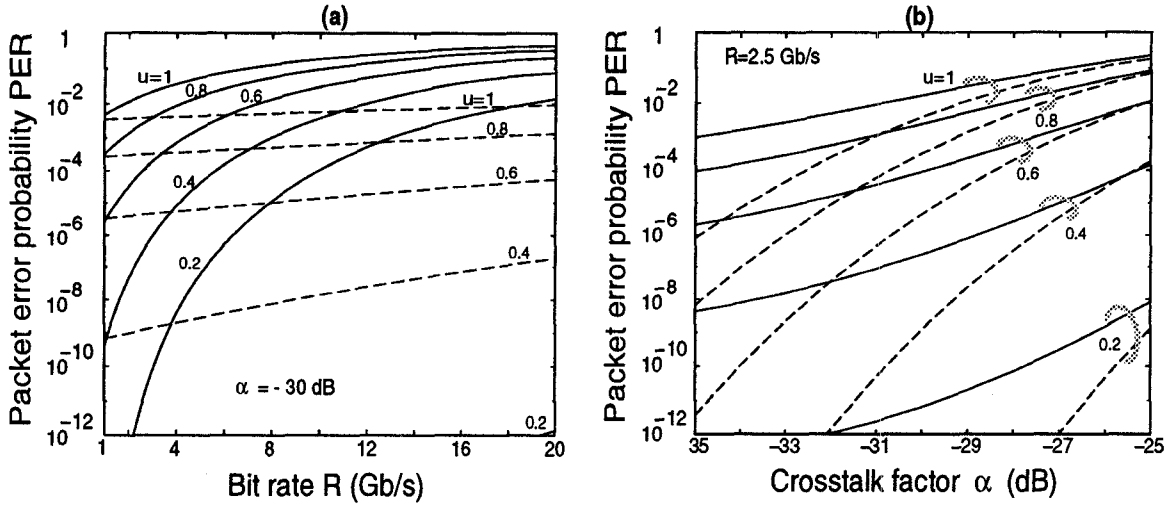

Figure 3: PER vs (a) bit rate R; (b) crosstalk factor α. Sold: single buffer, Dotted: no buffer.

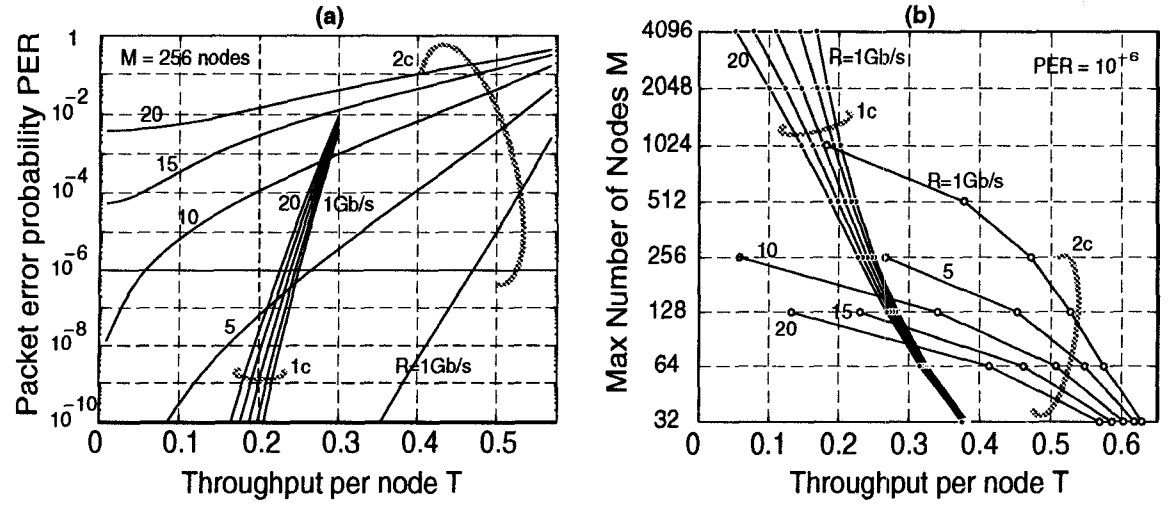

Figure 4: (a) PER vs throughput; (b) Maximum number of nodes vs throughput for $PER < 10^{-6}$.

Curves for $2c$ show instead a marked dependence on bit rate, which indicates that signal-ASE beat dominates. The different behavior is due to the doubling of power losses at the active star in the $2c$ case. From Fig 3(b) it can be observed that full load operation at 2.5 Gb/s with PER below 10^{-6} can only be achieved by $1c$ for crosstalk factor below -35 dB. The $2c$ interconnect cannot work at full load with PER below 10^{-6}, because of the excessive ASE noise. A floor for low values of α is in fact visible in the figure. Using the more complex $2c$ interconnect gives lower PER only at bit rates below a few Gb/s.

However, a comparison between $1c$ and $2c$ at equal value of u is unfair, since in such case $2c$ can sustain a much larger throughput (Fig. 2). Therefore a fair comparison should plot PER vs Throughput T. In fact, for a given transmitter bit rate R, T indicates the actual sustained rate R_a at the access node, since $T = R_a/R$.

PER vs throughput curves are given in Fig. 4(a), with R ranging from 1 to 20 Gb/s. The curves for $1c$ weakly depend on R, again indicating that coherent crosstalk is the dominant impairment. The curves for $2c$ have instead a strong variation with R. For a given T, this curve shows the advantage of using the simpler $1c$ interconnect at higher bit rates to deplete the optical layer and hence to lower u for a given offered rate R_a. If for instance $R = 5$ Gb/s, for all rates $R_a < 0.23R = 1.1$ Gb/s, $1c$ guarantees a lower PER than 2c, well below 10^{-6}; it is thus the best solution if it is cheaper to have fast TX/RXs than a more complex interconnect. For larger rates, up to $0.27R = 1.35Gb/s$, only $2c$ can guarantee $PER < 10^{-6}$. If the arrival rate is even larger, a faster TX must be used in both cases, say $R' = 10$ Gb/s, in which case $1c$ gives lower PER over essentially all its throughput range (0–0.27), and guarantees $PER < 10^{-6}$, up to arrival rates of $0.22R' = 2.2Gb/s$.

Slicing Fig. 4(a) at a target $PER = 10^{-6}$ and varying the number of nodes gives the performance scaling curves of Fig. 4(b). For example, it is seen that the only way to serve up to 1024 nodes at an effective rate $R_a = 1Gb/s$ is to use $1c$ β-elements and R=5Gb/s.

6 Conclusions

This work shows the conditions for transmission feasibility of "mildly" multihop all-optical single-wavelength networks. A control of the network load is necessary to avoid excessive error rates

at the receiver. The clear indication is that such transparent networks work best if lightly loaded at the optical level. This means that the cost burden must be shifted to speed-up the optical transmitter/receiver at the access node to allow major simplifications and cost reductions of the optical transport/switching part of the network.

Appendix

The constrained optimization problem can be recast as follows: find gains (G_1, G_3) such that $N_{ase}(n)$ in (6) is minimized, subject to the constraints

$$\begin{array}{rcl} \max(1,a) \leq & G_1 & \leq G_M \\ 1 \leq & G_3 & \leq G_M \\ \max(b,c) \leq & G_1 G_3 & \leq d \end{array} \qquad (21)$$

where $a = \frac{P_{tx}}{P_{sat}} \frac{L_f L_n}{L_{ad}}$, $b = a\, L_s$, $c = \frac{L_f^2 L_n L_s}{G_M}$, $d = c\, G_M$.

Fig. 5 shows an example of the above constraints, along with an indication of their physical meaning. The shaded area $\mathcal{D}$ is the domain of optimization. For $\mathcal{D}$ to be not empty, the following conditions must hold: $\max(b,c) \leq G_M^2$, $a < G_M$, $\max(b,c) < d$. Define the points: $A \equiv \left(\frac{\max(b,c)}{G_M}, G_M\right)$, $B \equiv \left(\max(a,1), \frac{\max(b,c)}{\max(a,1)}\right)$, $C \equiv (\max(a,1), 1)$.

When $\mathcal{D}$ is non-empty, if B is to the right of A and above C, i.e., when $\max(b,c) > \max(a,1) > \frac{\max(b,c)}{G_M}$, point B is the optimal point, since $(G_1 \cdot G_3)$ and G_1 reach simultaneously their minimum allowed values, thereby minimizing $N_{ase}(n)$. In such case the optimal gains are $(G_1, G_2, G_3) = (\max(a,1), \frac{cG_M}{\max(b,c)}, \frac{\max(b,c)}{\max(a,1)})$.

If B is instead to the left of A, i.e., $\frac{\max(b,c)}{G_M} > \max(a,1)$, then the optimal point is A, and the corresponding gains are $(G_1, G_2, G_3) = (\frac{\max(b,c)}{G_M}, \frac{cG_M}{\max(b,c)}, G_M)$.

Finally, if B is below C, i.e., $\max(a,1) > \max(b,c)$, which corresponds to an unlikely situation in which losses are very low, the optimal point is C, and the gains are $(G_1, G_2, G_3) = (\max(a,1), \frac{cG_M}{\max(a,1)}, 1)$, i.e., amplifier A_3 is not needed.

For example, for the values in Table 1, we get that for 1c the optimal point is B (medium losses), the optimal gains are $(G_1, G_2, G_3) = (0, 11.5, 24.5)$(dB), and $N_{ase}(1) = 1.07 \times 10^{-17}$(W/Hz); for 2c the optimal point is A (large losses), the gains are $(G_1, G_2, G_3) = (10.5, 11.5, 30)$(dB), and $N_{ase}(1) = 4.18 \times 10^{-16}$(W/Hz).

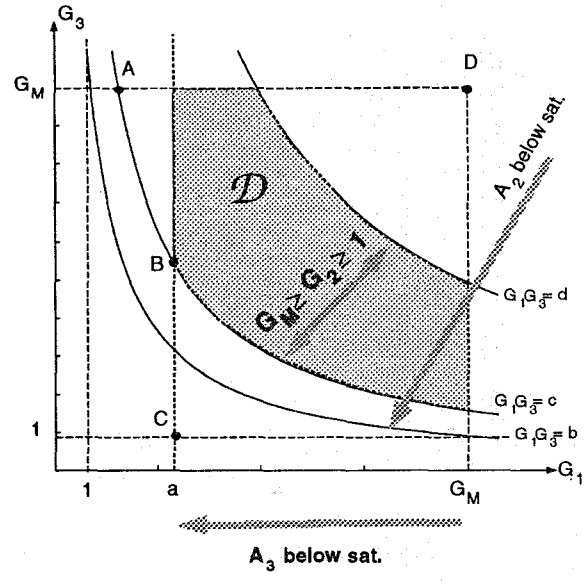

Figure 5: Gain optimization domain D

References

[1] E. L. Goldstein and L. Eskildsen, "Scaling limitations in transparent optical networks due to low-level crosstalk," *IEEE Photon. Technol. Lett.*, vol. 7, pp. 93–94, Jan. 1995.

[2] A. Bononi, "Space-division optical star networks with deflection routing," *30th Annual Conference on Information Science and Systems*, session FA-1, Princeton, NJ, March 20–22, 1996.

[3] F. Forghieri, A. Bononi, and P. R. Prucnal, "Analysis and comparison of hot-potato and single-buffer deflection routing in very high bit rate optical mesh networks," *IEEE Trans. Commun.*, vol. 43, pp. 88–98, Jan. 1995.

[4] P. Baran, "On distributed communications networks," *IEEE Trans. Commun. Syst.* vol. 12, pp. 1–9, Mar. 1964.

[5] N. F. Maxemchuk, "Comparison of deflection and store-and-forward techniques in the Manhattan Street and Shuffle-Exchange networks," in *Proc. IEEE INFOCOM '89*, pp. 800–809, Apr. 1989.

[6] O. K. Tonguz and L. G. Kazovsky, "Theory of direct-detection lightwave receivers using optical amplifiers," *IEEE J. Lightwave Technol.*, vol. 9, pp. 174–181, Feb. 1991.

[7] R. R. Ramaswami and P. A. Humblet, "Amplifier induced crosstalk in multichannel optical networks," *IEEE J. Lightwave Technol.*, vol. 8, pp. 1882–1896, Dec. 1990.

[8] N. A. Olsson, "Lightwave systems with optical amplifiers," *IEEE J. Lightwave Technol.*, vol. 7, pp. 1071–1082, July 1989.

[9] P. A. Humblet and M. Azizoglu, "On the bit error rate of lightwave systems with optical amplifiers," *IEEE J. Lightwave Technol.*, vol. 9, pp. 1576–1582, Nov. 1991.